Replica exchange enveloping distribution sampling (RE-EDS): A robust method to estimate multiple free-energy differences from a single simulation

Sidler, Dominik ; Schwaninger, Arthur ; Riniker, Sereina

DOI: https://doi.org/10.1063/1.4964781

The Journal of Chemical Physics

Replica exchange enveloping distribution sampling (RE-EDS): A robust method to estimate multiple free-energy differences from a single simulation

Cite as: J. Chem. Phys. **145**, 154114 (2016); https://doi.org/10.1063/1.4964781
Submitted: 04 August 2016 . Accepted: 30 September 2016 . Published Online: 19 October 2016

Dominik Sidler, Arthur Schwaninger, and Sereina Riniker

AIP Publishing

Replica exchange enveloping distribution sampling (RE-EDS): A robust method to estimate multiple free-energy differences from a single simulation

Dominik Sidler, Arthur Schwaninger, and Sereina Riniker[a)]
Laboratory of Physical Chemistry, ETH Zürich, Vladimir-Prelog-Weg 2, 8093 Zürich, Switzerland

(Received 4 August 2016; accepted 30 September 2016; published online 19 October 2016)

In molecular dynamics (MD) simulations, free-energy differences are often calculated using free energy perturbation or thermodynamic integration (TI) methods. However, both techniques are only suited to calculate free-energy differences between two end states. Enveloping distribution sampling (EDS) presents an attractive alternative that allows to calculate multiple free-energy differences in a single simulation. In EDS, a reference state is simulated which "envelopes" the end states. The challenge of this methodology is the determination of optimal reference-state parameters to ensure equal sampling of all end states. Currently, the automatic determination of the reference-state parameters for multiple end states is an unsolved issue that limits the application of the methodology. To resolve this, we have generalised the replica-exchange EDS (RE-EDS) approach, introduced by Lee *et al.* [J. Chem. Theory Comput. **10**, 2738 (2014)] for constant-pH MD simulations. By exchanging configurations between replicas with different reference-state parameters, the complexity of the parameter-choice problem can be substantially reduced. A new robust scheme to estimate the reference-state parameters from a short initial RE-EDS simulation with default parameters was developed, which allowed the calculation of 36 free-energy differences between nine small-molecule inhibitors of phenylethanolamine *N*-methyltransferase from a single simulation. The resulting free-energy differences were in excellent agreement with values obtained previously by TI and two-state EDS simulations. *Published by AIP Publishing.* [http://dx.doi.org/10.1063/1.4964781]

I. INTRODUCTION

Rigorous methods to estimate free-energy differences that rely on conformational sampling from molecular dynamics (MD) or Monte Carlo (MC) simulations belong to the most accurate but also computationally expensive approaches.[1,2] In these methods, both enthalpic and entropic contributions are considered explicitly, as well as solvent effects if treated accordingly. However, this involves an exhaustive sampling of each end state, as well as proper sampling of the transition pathway in-between. The most popular techniques such as thermodynamic integration (TI)[3] or free energy perturbation (FEP)[4] are pathway methods for two-state systems. For each pair of end states a separate TI or FEP calculation must be performed, which can become cumbersome if a large number of end states are investigated (e.g., series of ligands for a particular protein target). Approaches such as the lead optimisation mapper[5] used in large-scale FEP calculations of binding free energies were developed to reduce the combinatorial explosion, but the estimation of multiple free-energy differences from a single simulation would be even more efficient. In enveloping distribution sampling (EDS),[6–9] a reference-state Hamiltonian H_R is sampled which "envelopes" the Hamiltonians of the end states. The approach allows in principle to sample $N \geq 2$ end states in a single simulation, and is thus potentially computationally more efficient than strictly two-state approaches. The reference state can be tuned to optimise sampling of all end states using two sets of parameters: the smoothness parameter(s) s and the energy offsets E_i^R. The smoothness parameter s allows to flatten the complex landscape of V_R, i.e., small s-values allow transitions between the different end states. The energy offsets allow to modify the contribution of each end state i to V_R individually. However, the choice of the involved $N + 1$ (or more) parameters of the reference state turned out to be a non-trivial task, which is why a robust parameter estimator is only known for two-state systems, for which the computational effort is comparable to TI.[10] Consequently, the full potential of EDS has not yet been exhausted.

The combination of Hamiltonian replica exchange (H-RE)[11–13] with EDS (RE-EDS) has recently been proposed in the context of constant-pH MD to switch between discrete protonation states.[14,15] RE-EDS allows to reduce significantly the complexity of the problem to choose optimal reference-state parameters. In constant-pH MD, the energy offsets are given by the pH, the pK_a of the model compound and the protonation free energy of the model compound in solution.[14] This approach is thus limited to these types of systems and cannot be used generally. In this study, we generalise the RE-EDS technique to calculate free-energy differences between any end states. A new robust scheme to estimate the reference-state parameters from a single initial RE-EDS simulation with default parameters is developed. Initial tests of RE-EDS are carried out with a test system of five dis-/

a)Electronic mail: sriniker@ethz.ch. URL: www.riniker.ethz.ch.

appearing water molecules as used previously in Refs. 7 and 8. The methodology and the new estimation scheme are further tested using different subsets of ten small-molecule inhibitors of phenylethanolamine *N*-methyltransferase (PNMT) in water. This is a challenging ligand series with diverse functional groups, including a deprotonated carboxy group which leads to a change in net charge.

II. THEORY

A. Enveloping distribution sampling (EDS)

Enveloping distribution sampling (EDS) is based on a reference state R, which combines N end states into one Hamiltonian (the kinetic part is omitted for simplicity),[7,16,17]

$$V_R(\mathbf{r}, s, \vec{E}^R) = -(\beta s)^{-1} \ln\left\{ \sum_{i=1}^{N} e^{-\beta s (V_i(\mathbf{r}) - E_i^R)} \right\}, \tag{1}$$

where s is the smoothness parameter and E_i^R are the energy offsets.[7] In this form, the reference state has $N+1$ parameters, $\{E_1^R, \ldots, E_N^R, s\} = \{\vec{E}^R, s\}$. Alternative reference state Hamiltonians with pairwise smoothness parameters s_{ij} have been proposed as well.[9] The free-energy difference between two end states i and j can then be calculated as

$$\Delta G_{ji} = -\beta^{-1} \ln \frac{\left\langle e^{-\beta(V_j - V_R)} \right\rangle_R}{\left\langle e^{-\beta(V_i - V_R)} \right\rangle_R}. \tag{2}$$

The effect of the energy offsets on V_R can be interpreted pictorially as a change of the depth of local minima corresponding to end state i.[10] However, since V_R in Eq. (1) cannot be separated into a sum over N terms that only depends on E_i^R and s, the validity of this interpretation may depend on the end states i (i.e., the phase space overlap between each end state has to be taken into account). Therefore, a change of E_i^R cannot only affect the local minimum corresponding to end state i but also the local minimum corresponding to end state j in V_R, which increases the difficulty to choose appropriate energy offsets.

If the $N+1$ reference-state parameters were chosen optimally, V_R allows transitions between N end states and hence sufficient sampling of all end states is obtained. In other words, by simulating an optimal V_R it is possible to calculate $\binom{N}{2}$ free-energy differences from a single simulation using ensemble reweighting (Eq. (2)). The main challenge in EDS is therefore the choice of the reference-state parameters. An ideal approach fulfills the following three conditions: (i) sampling of physically accurate configurations, (ii) robust parameter choice for more than two end states, and (iii) low computational cost. Two different iterative schemes were proposed in the past to estimate the reference-state parameters automatically.[7,8,10] Starting from initial guesses for the parameters, short EDS simulations were performed iteratively until convergence, updating the parameters after each run. The first heuristic scheme is applicable to $N \geq 2$ end states,[7,8] but exhibits an artificial reciprocal dependence on the energy offsets, which leads to underestimated s-values for large energy-offset differences.[10] The second scheme is based on a decision tree, which resolves the issue of the first approach at the cost of restricting the application of EDS to two end states.[10] In both cases, the double-iterative nature increases the computational cost.

B. Replica exchange (RE)

Replica exchange (RE)[11] is a popular approach to enhance sampling in MD simulations. Two main variants are known: (i) temperature replica exchange[18] (T-RE) and (ii) Hamiltonian replica exchange (H-RE), which is typically used in combination with TI.[12,13]

For H-RE, the probability to accept the exchange is given as

$$p_{\text{acc}} = \min\left[1, e^{-\Delta}\right], \tag{3}$$

$$\Delta := \beta\left\{\left[V(\zeta_i, \mathbf{r_j}) + V(\zeta_j, \mathbf{r_i})\right] - \left[V(\zeta_i, \mathbf{r_i}) + V(\zeta_j, \mathbf{r_j})\right]\right\}, \tag{4}$$

where $\beta = 1/k_B T$, k_B is the Boltzmann constant, T is the temperature, V the potential energy, $\mathbf{r_i}$ the configuration of replica i, and ζ the varying parameter between replicas.

C. Replica-exchange EDS (RE-EDS)

1. Concepts and assumptions

A way to fulfil the three conditions listed above is replica-exchange EDS (RE-EDS). By employing replicas at different s-values and exchanging configurations between them, no single optimal value for s is required as long as values below and above were chosen for the replicas (Fig. 1(a)). The physical accuracy of the simulation can be guaranteed by taking into account only data obtained at high s-values ($s \approx 1$), whereas small s-values are needed to obtain transitions between the various end states. The parameter-estimation problem reduces thus largely to the problem of obtaining appropriate energy offsets.

Both previously proposed schemes to choose reference-state parameters use the same heuristic approach to estimate the energy offsets,[7]

$$E_i^R(new) = -\frac{1}{\beta} \ln \left\langle \left[1 + \sum_{\substack{j=1 \\ j \neq i}}^{N} e^{-\beta\left(\Delta V_{ji} - \Delta E_{ji}^R\right)} \right]^{-1} \right\rangle_{R(s, \vec{E}^R(old))} + E_i^R(old). \tag{5}$$

Previous simulations showed that at small s-values, so-called "undersampling" occurs, i.e., the important configurations of the end states are no longer completely sampled but instead unphysical intermediate configurations, which are favourable for all end states enveloped in a reference state.[10] In addition, it was observed that although the smoothness parameters can differ up to two orders of magnitude between the two parameter-estimation schemes, similar estimates for the energy offsets were obtained for two-state systems using Eq. (5).[10] This indicates that Eq. (5) possibly depends only weakly on the chosen s-value, as long as all end states are at least partially visited.

Combining the aforementioned two observations allows to decouple the problem of choosing optimal E_i^R values from the problem of choosing an optimal s-value. Thus, the

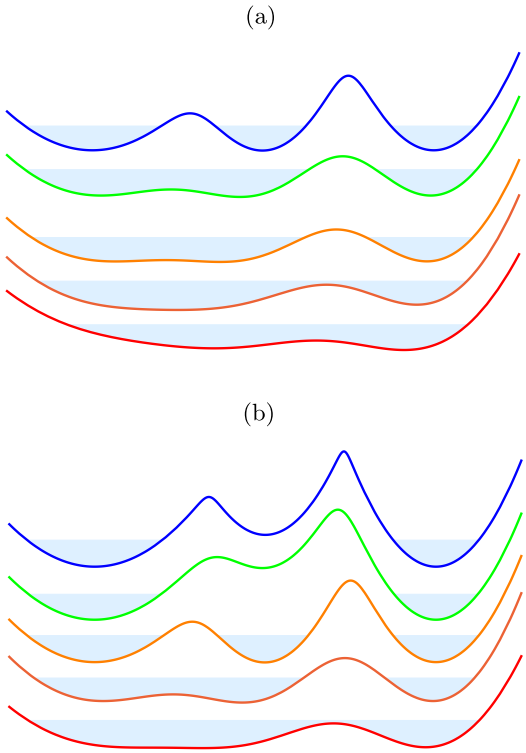

FIG. 1. Schematic representation of the reference-state Hamiltonian in a RE-EDS simulation for different parameter choices (s, $\vec{E}^R$). The reference state in one dimension was constructed from three different harmonic oscillator potentials $V_1 := 10x^2$, $V_2 := 10(x-2)^2 + 4$, and $V_3 := 4(x+2)^2 - 2$. The regions shaded in light blue visualize configurations which are accessible at a given temperature T. The horizontal axis indicates system coordinates and each coloured line corresponds to a reference state with increasing s-value from bottom to top (red: smallest s-value, blue: highest s-value). (a) Ideal RE-EDS setup. (b) "Leakage" of good exchanges.

energy offsets $E_i^R(new)$ can possibly be estimated for every s small enough such that "undersampling" occurs, without having to know the energy offsets in advance. However, if the decoupling is not valid and thus the energy offsets are not chosen well, "leakage" effects may occur as illustrated in Fig. 1(b), which prevents that all end states are sampled at high s-values.

Note: A good performance of RE-EDS requires that sufficient configuration exchanges using the Boltzmann acceptance criterion (Eq. (4)) occur, such that all end states are visited within a finite time scale. This is not obvious *a priori* since V_R depends in a nonlinear fashion on s. Therefore, a small change in s can possibly modify the shape of the potential surface substantially, leading to low Boltzmann acceptance probabilities, which demands a system-dependent optimisation of the s-value distribution.

2. General scheme to estimate energy offsets

Based on the assumptions mentioned above, we define a general approach to estimate energy offsets for multiple states in the following.

(i) A short initial RE-EDS simulation with M smoothness parameters $s \in S := \{s_j \in (0,1] \mid s_j < s_{j+1}, j \in [M]\}$ is performed. The N energy offsets are set to zero for all replicas, i.e., $E_i^R = 0$. For simplicity, the same starting configuration is used for all replicas. The first n time steps are discarded as equilibration to avoid any bias from the starting configuration.

(ii) The heuristic estimator[7] (Eq. (6)) is solved iteratively for each replica $s \in S$ until convergence, i.e., until $\sum_i \left(E_i^R(\text{new}) - E_i^R(\text{old})\right) < \rho$, where ρ corresponds to a convergence radius.

$$E_i^R(new) := -\frac{1}{\beta} \ln \left\langle e^{-\beta\left(V_i(\mathbf{r}) - V_R(s \stackrel{!}{=} 1, \vec{E}^R(old))\right)} \right\rangle_{R(s,\vec{E}^R(old))}. \quad (6)$$

After each iteration, the energy offset of one end state is set to zero, e.g., $E_1^R = 0$, and the other energy offsets are set to their relative values. This constraint is necessary to obtain fast convergence when solving Eq. (6). In practice, the solution of Eq. (6) did not show any dependency on which particular energy offset E_i^R was kept fixed at zero (i.e., $E_j^R - E_k^R \approx const$, $\forall i,j,k$ with $E_i^R \stackrel{!}{=} 0$).

(iii) The s-values where "undersampling" occurs are identified. For this, we define a region $U := \{s \in S \mid b_i(s) > f_{th}, \forall i \in [N]\}$, where $f_{th} \in [0,1]$ is a user-defined threshold fraction. To this end, the number of low-energy configurations $b_i(s)$ are calculated for each end state i and $s \in S$,

$$b_i(s) := \frac{\sum_t \mathcal{H}(V_{th} - V_i(s,t))}{\sum_t 1}, \quad (7)$$

where $\mathcal{H}$ corresponds to the Heaviside step function. Thus, Eq. (7) counts the fraction of conformations for which the potential energy of end state i, $V_i(s,t)$, is below a user-defined threshold potential energy V_{th}.

The two parameters V_{th} and f_{th} were introduced as a measure to decide whether "undersampling" occurs at a given s-value (=replica), i.e., if the sampled configuration corresponds to an intermediate state, which is favourable for all end states.[10] The definition makes implicitly use of the fact that if a configuration is unfavourable for a state i, the corresponding potential energy will be very high due to unfavourable van der Waals interactions, i.e., $V_i \gg V_{th}$.

(iv) The energy offsets obtained in step (iii) are averaged over all s-values belonging to the "undersampling" region U in order to increase the robustness of the energy offset estimator,

$$\bar{E}_i^R := \sum_{s \in U} \frac{E_i^R(new)(s)}{|U|}. \quad (8)$$

Some additional remarks: It can be shown that Eq. (6) is equivalent to Eq. (5), introduced by Christ *et al.*[8] Furthermore, using Eq. (2) shows that for $s = 1$ the energy offset of state i corresponds to the free-energy difference between state i and the reference state (assuming proper sampling of V_R),

$$E_i^R(s \stackrel{!}{=} 1) = \Delta G_{iR}. \quad (9)$$

In order to understand the effect of the smoothness parameter s on the dynamics of the system, one can investigate the limiting behaviour of the force acting on a single

particle as given in the Appendix. Suppose $s \to 0$, it can be shown that simulating the corresponding reference state is equivalent to the parallel simulation of all solute states in one solvent environment (Eq. (A3)), where the interaction between different solutes is not taken into account, but the solute-solvent interaction is considered for every solute. Therefore, a solvent conformation which is suitable for all end states will be sampled in the "undersampling" region at every time step. On the contrary, for high s-values the solute-solvent interaction will tend towards the non-smoothed value of the currently occupied end state as can be seen for $s \to \infty$ in the Appendix (Eq. (A4)). Therefore, for $s \to \infty$ the simulation corresponds to the setup of one solute in solvent only. Theoretically, at $s = 1$, the sampling of V_R has to be considered as an intermediate state, with a biased potential surface for each end state i compared to a simulation of V_i only. However, for the given system in water, the pairwise energy offset scheme[10] already showed high physical accuracy for substantially lower s-values. Hence, $s = 1$ was considered to be sufficiently physically accurate in practice and was therefore used as an upper limit in the RE-EDS simulations.

III. METHODS

A. Simulation protocols

All RE-EDS simulations were performed using a modified version of the GROMOS program package[19,20] with the 53A6 GROMOS force field[21] and the simple-point charge (SPC)[22] water model. In all simulations, a twin-range method was used for the non-bonded interaction calculations with cutoff radii of 0.8 nm (short-range) and 1.4 nm (long-range), where the pairlist for pairs within the short range cutoff and the energies and forces for long-range pairs were updated every 10 fs (5 steps). The force from atoms beyond the long-range cutoff was mimicked using a reaction field correction[23] due to a continuum approximation with a relative dielectric permittivity ϵ_{rf} of 61.[24] The integration time step was 2 fs.

1. Five dis-/appearing water molecules

A system consisting of five solute water molecules in water was used as a simple test system as previously described in Refs. 7 and 8. In each of the five end states, one of the solute water molecules was interacting with the solvent, whereas the other four solute water molecules were perturbed to "dummy," i.e., they were not interacting with other particles in the system. This setup of "creating" and "annihilating" water molecules in water creates large potential wells between the end states in the reference-state potential. Since the solute-solvent interactions are equal for all five end states, the energy offsets are zero and the resulting free-energy differences as well, making it a good test system for the RE-EDS setup.

The RE-EDS setup for the dis-/appearing water system consisted of 21 different s-values, which were chosen logarithmically distributed between 1 and 0.001. All energy offsets were set to zero (i.e., $E^R_{i,0} = 0$). 250 replica-exchange attempts were made with an interval of 6 ps, resulting in a total simulation time of 1.5 ns. The system temperature was kept at 303.15 K for each replica by weak-coupling to a temperature bath with a coupling time of 0.1 ps.[25] The box volume was kept constant (NVT). The centre of mass motion was stopped every 2 ps (1000 steps). The five solute water molecules were solvated in a periodic, cubic box with 2737 SPC water molecules. The starting coordinates for the system were taken from an equilibrated 2742 SPC water box and the five solute molecules were selected randomly.

2. Phenylethanolamine N-methyltransferase inhibitors

The free-energy differences between a series of ten tetrahydroisoquinoline derivates (Fig. 2) were investigated, which were previously studied using TI[26] and two-state (or pairwise) EDS.[10] These compounds are inhibitors for phenylethanolamine N-methyltransferase (PNMT). The force field parameters for the ligands were taken from Ref. 26. All charges and atom types used can be found in Table S1 in the supplementary material of Ref. 10. All relevant system parameters were chosen identical to Ref. 10 such that the results could be directly compared. Thus, the contribution of the excluded atoms to the reaction field was not considered as done in older versions of GROMOS.

The system temperature was kept at 298 K for each replica by weak-coupling to a temperature bath with a coupling time of 0.1 ps.[25] The pressure was constrained at 1 atm by a similar type of algorithm using a coupling time of 0.5 ps and an isothermal compressibility of $4.575 \cdot 10^{-4}$ (kJ mol^{-1} nm^{-3})$^{-1}$. The center of mass motion was stopped every 20 ps (10 000 steps).

The starting conformations were taken from Ref. 10. The ligands were solvated in a periodic, cubic box with

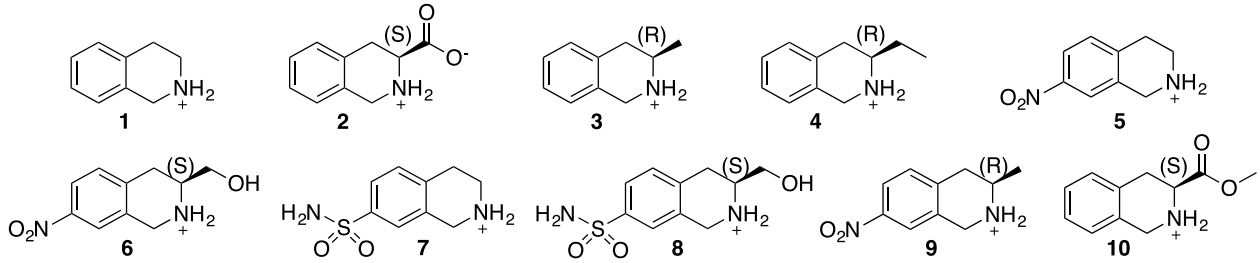

FIG. 2. Ten tetrahydroisoquinoline derivates which are inhibitors of phenylethanolamine N-methyltransferase (PNMT).

TABLE I. Average potential energy of the ten PNMT inhibitors obtained from 2-ns standard simulation of each ligand i in SPC water.

Ligand i	$\bar{V}_i^{\text{non-EDS}}$ (kJ/mol)
1	−370
2	−801
3	−378
4	−387
5	−394
6	−447
7	−822
8	−877
9	−403
10	−524

TABLE II. Energy offsets E_i^R for the five PNMT inhibitors **1**, **4**, **6**, **7**, and **10** in water. The average potential energies were obtained from 2-ns standard simulations of the individual ligands (Table I): $E_{i,\text{pot}}^R = \bar{V}_i^{\text{non-EDS}} - \bar{V}_1^{\text{non-EDS}}$. The pairwise energy offsets $E_{i,\text{pair}}^R$ were taken from Ref. 10. The energy offsets of the new scheme, $\bar{E}_{i,RE}^R$, were obtained by averaging over the replicas with "undersampling." The root-mean-square deviation of the average was computed as an error estimate.

Ligand i	$E_{i,0}^R$ (kJ/mol)	$E_{i,\text{pot}}^R$ (kJ/mol)	$E_{i,\text{pair}}^R$ (kJ/mol)	$\bar{E}_{i,RE}^R$ (kJ/mol)
1	0	0	0	0
4	0	−17	−6.2	−12.8 ± 4.3
6	0	−77	−42.5	−45.2 ± 4.7
7	0	−452	−353.8	−348.4 ± 16.8
10	0	−154	−133.8	−134.1 ± 7.7

975 SPC water molecules. A dual-topology representation together with distance restraints between four carbons of the benzene moiety (force constant $K = 1000$ kJ mol^{-1} nm^{-2} and ideal distance $r_0 = 0.0$ nm) was applied analogously to Ref. 10.

Three subsets of the ten ligands (Fig. 2) were studied. The first subset consisted of five ligands **1**, **4**, **6**, **7**, and **10**, which was used as a test system to develop the new scheme for estimating the energy offsets. The second subset consisted of nine ligands **1**, **3**, **4**, **5**, **6**, **7**, **8**, **9**, and **10**, whereas in the third subset all ten ligands were combined. Note that ligand **2** has a net charge of zero due to a deprotonated carboxy substituent while the other nine ligands are positively charged.

For analysis purposes, standard simulations of the individual ligands in water were carried out for 2 ns using identical system parameters as described above for the RE-EDS simulations (Table I).

In total five different RE-EDS simulations of 25 ns length were performed for the five-state system. Four different sets of energy offsets were used as listed in Table II, with 21 s-values distributed logarithmically between 1 and 0.001. An additional simulation was carried out with $E_{i,0}^R$ and a manually optimized s-value distribution: $s \in S_{0,\text{opt}}^5 := \{1, 0.5, 0.25, 0.13, 0.063, 0.031, 0.022, 0.0188, 0.016, 0.141, 0.0125, 0.011, 0.0093, 0.008, 0.0066, 0.0057, 0.0047, 0.004, 0.0028, 0.002, 0.001\}$. The optimization was based on the replica-exchange acceptance probabilities in the first 2.5 ns of the run with logarithmically distributed s-values. In all five simulations, the frequency of replica-exchange attempts was 10 ps.

The energy offsets based on average potential energies were obtained from the 2-ns standard simulations of the individual ligands (Table I) by calculating $E_{i,\text{pot}}^R := \bar{V}_i^{\text{non-EDS}} - \bar{V}_1^{\text{non-EDS}}$. The pairwise energy offsets $E_{i,\text{pair}}^R$ were taken from Ref. 10. In order to estimate the RE-EDS energy offsets $\bar{E}_{i,RE}^R$ for the five-state system, simulation data from the first 5 ns of the $E_{i,0}^R$ run with manually optimised s-values were taken. To avoid any bias of the estimator due to a non-optimal starting configuration, the first 2.5 ns was discarded as equilibration. Theoretically, a much shorter equilibration time would be sufficient. In the estimation scheme, the threshold potential energy was set to $V_{th} = 0$ and a threshold fraction of $f_{th} = 0.5$ was chosen, resulting in an energy offset $\bar{E}_{i,RE}^R$ averaged over the values of $E_{i,RE}^R$ taken from the smallest 12 s-values. The convergence radius ρ was set to 1.0 to solve Eq. (6) iteratively.

In order to estimate the RE-EDS energy offsets for the nine-state system, an initial RE-EDS simulation of 4.5 ns length with no energy offsets $E_{i,0}^R$ and 21 s-values

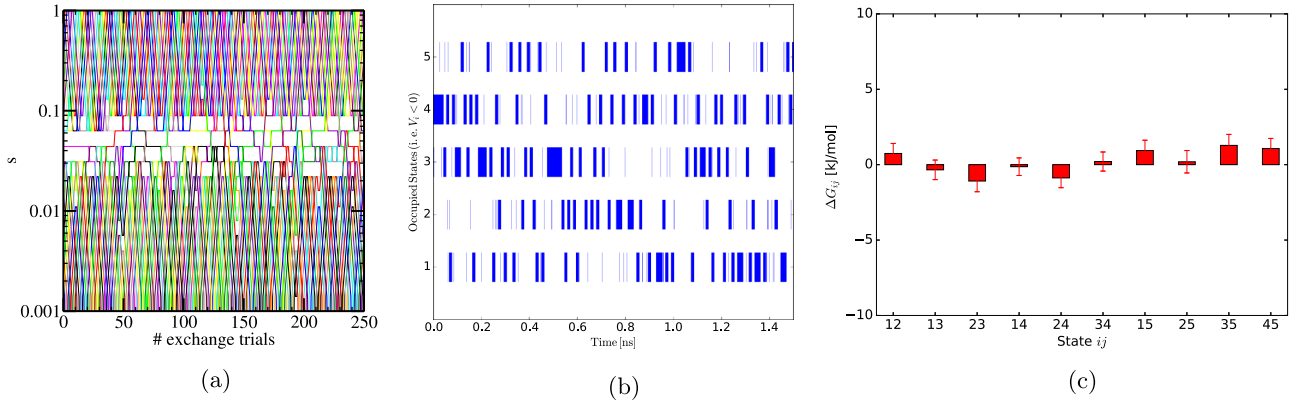

FIG. 3. RE-EDS simulation of five dis-/appearing water molecules in water using 21 logarithmically distributed s-values and all energy offsets set to zero. (a) Replica-exchange attempts in the 1.5 ns simulation. (b) Occupancy of the five end states at $s = 1$. (c) Free-energy differences between all five end states obtained from the 1.5 ns simulation. The error bars shown are statistical uncertainties.[7] The reference value for ΔG_{ij} is 0.0 kJ/mol.

logarithmically distributed between 1 and 0.001 was carried out. The first 1.5 ns were discarded as equilibration in order to avoid any influence of the initial configuration. The threshold potential energy was set to $V_{th} = 0$ and a threshold fraction of $f_{th} = 0.5$ was chosen, resulting in averaged energy offsets $\bar{E}^R_{i,RE}$, based on the eight smallest s-values of the initial RE-EDS simulation. The convergence radius was set to $\rho = 1.0$ for the iterative procedure. The resulting RE-EDS energy offsets are listed in Table IV. Using these energy offsets, two production runs of 30 ns length were performed. In the first run, 21 replicas with logarithmically distributed s-values between 1 and 0.001 were used. For the second run, the s-value distribution was manually optimised based on the acceptance probabilities of the first run (see Fig. 7). The resulting set of 24 optimised s-values was $S^9_{\mathrm{RE,opt}} := \{1, 0.6, 0.35, 0.25, 0.18, 0.13, 0.101, 0.089, 0.073, 0.063, 0.052, 0.044, 0.036, 0.031, 0.026, 0.022, 0.0185, 0.016, 0.013, 0.011, 0.008, 0.004, 0.002, 0.001\}$. The frequency of the replica-exchange attempts was 10 ps in all cases.

The RE-EDS energy offsets for the ten-state system including ligand **2** (Table IV) were calculated identically to the energy offsets of the nine-state system.

B. Analysis

In order to analyse the obtained simulation data, analysis programs from GROMOS++[27] were used. The desired simulation properties were extracted from the energy trajectories with *ene_ana*. The free-energy differences were calculated by reweighting according to Eq. (2) with *dfmult*. The potential-energy distributions were generated with *tcf*.

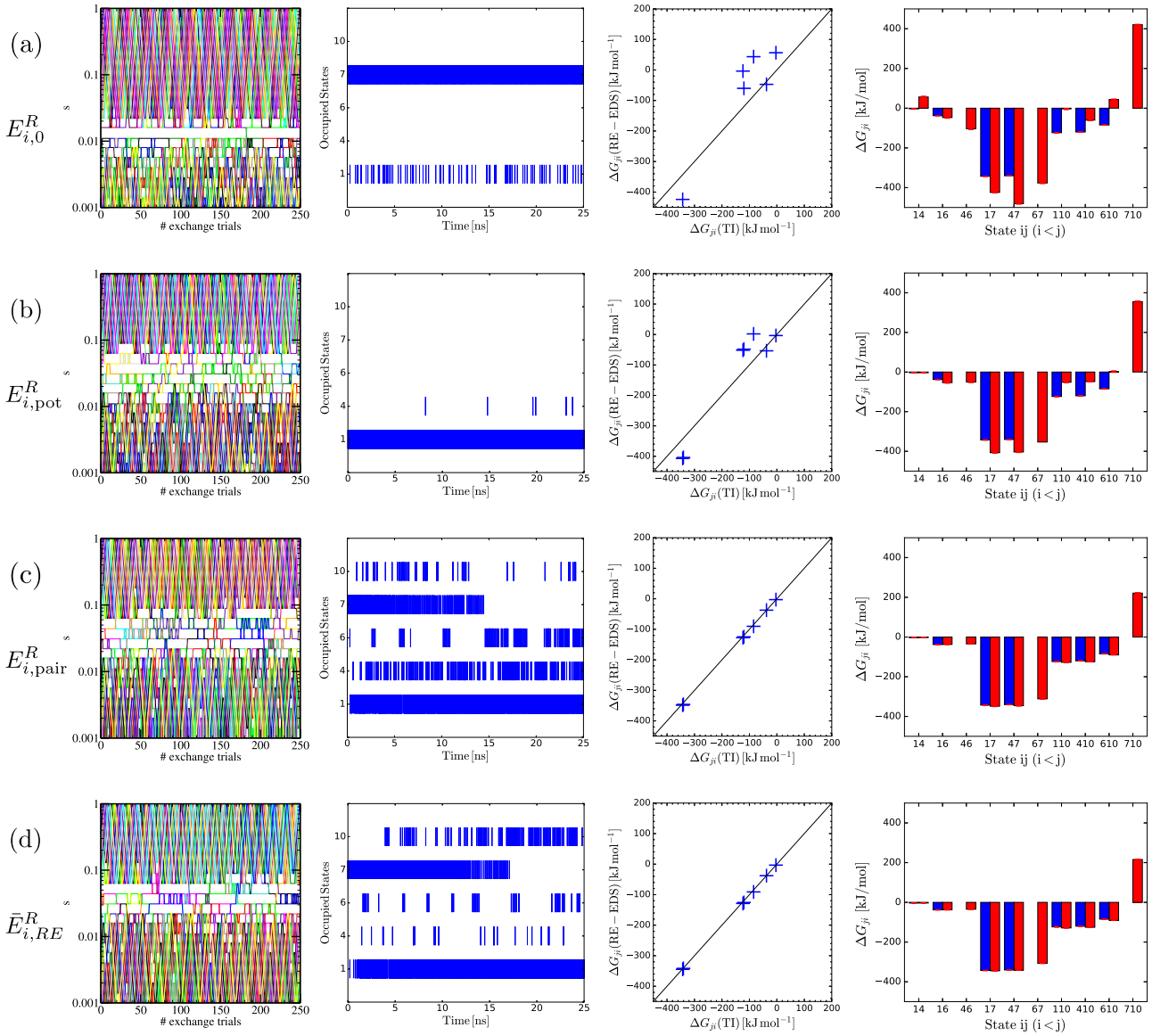

FIG. 4. RE-EDS simulation of the five PNMT inhibitors **1**, **4**, **6**, **7**, and **10** in water with 21 logarithmically distributed s-values. The energy offsets are chosen differently from top to bottom: $\{E^R_{i,0}, E^R_{i,\mathrm{pot}}, E^R_{i,\mathrm{pair}}, \bar{E}^R_{i,RE}\}$. All simulations were performed for 25 ns. From left to right: (i) replica-exchange attempts during the first 2.5 ns of simulation time, (ii) occupation of ligand i with respect to time t (i.e., $V_i < \bar{V}_i^{\mathrm{non-EDS}}$), (iii) comparison of the free-energy differences ΔG_{ji} obtained by RE-EDS and TI,[10] and (iv) all free-energy differences ΔG_{ji} of the five state system obtained by RE-EDS (red bars) and TI (blue bars).

The radial distribution functions (RDF) were computed with *rdf*.

In addition, a measure was introduced to assign a certain reference-state configuration at time t, $\mathbf{r}_R(t)$, to one (or more) end states. For this purpose, we defined the reference state to occupy end state i at time t if

$$V_i(\mathbf{r}_R(t)) < \bar{V}_i^{\text{non-EDS}}, \tag{10}$$

where $\bar{V}_i^{\text{non-EDS}}$ corresponds to the average potential energy obtained from a standard simulation of ligand i as given in Table I. In the calculation of $V_i(\mathbf{r}_R(t))$, the atoms of the other end states are included as dummies. Note that for finite s-values the phase space of the ligands can overlap in the (RE-)EDS setup, thus there is no unique assignment $\mathbf{r}_R \mapsto i$ possible in general. Therefore, a given configuration $\mathbf{r}_R(t)$ can be favourable (i.e., fulfilling Eq. (10)) for more than one end state at the same time. This intrinsic property allows a more efficient sampling of the EDS reference state compared to TI simulations.

In order to evaluate the robustness of the new energy-offset estimation scheme, the time evolution of the estimator as well as the dependence on the smoothness parameter s was investigated. To this end, the absolute evolution and relative evolution of the energy-offset estimation, compared to the estimator for a reference time frame $[t_0, t_{\text{ref}}]$, were computed as a function of time ($t \geq t_{\text{ref}}$), as follows:

$$\Delta E^R_{i,\text{abs}}(t) := \bar{E}^R_{i,RE}(t_0, t_{\text{ref}}) - \bar{E}^R_{i,RE}(t_0, t), \tag{11}$$

$$\Delta E^R_{i,\text{rel}}(t) := \frac{\Delta E^R_{i,\text{abs}}(t)}{\bar{E}^R_{i,RE}(t_0, t_{\text{ref}})}. \tag{12}$$

A similar comparison for the smoothness parameter s was defined in order to investigate the sensitivity of the averaged energy-offset estimates $\bar{E}^R_{i,RE}$ with respect to the ones obtained from a single s-value $E^R_{i,RE}(s)$,

$$\Delta E^R_{i,\text{abs}}(s) := E^R_{i,RE}(s) - \bar{E}^R_{i,RE}. \tag{13}$$

IV. RESULTS AND DISCUSSION

A. Five dis-/appearing water molecules

The simple test system of five dis-/appearing water molecules in water offers two important insights into the RE-EDS approach. First, a set of intermediate s-values was observed, for which the replica-exchange acceptance probability is significantly reduced (Fig. 3(a)). This region in s-space is termed "gap region" in the following. At s-values above and below the gap region, on the other hand, the replica-exchange acceptance probability was found to be close to one. For s-values below the gap region, undersampling occurs, whereas the reference-state potential is not smoothed at high s-values (i.e., distinct end states are sampled). Interestingly, the optimal s-value = 0.0657 determined in Ref. 8 for the same system lies within the gap region. These observations indicate that in the gap region the reference-state potential energy surface alters significantly between neighbouring replicas. In addition, as shown in Fig. S1 in the supplementary material, an increase in the number of end states N appears to broaden the gap region towards lower s-values for this system.

Second, the simple test system shows that all states were sampled equally at $s = 1$ with RE-EDS (Fig. 3(b)). Thus, the small s-values facilitate indeed transitions between the end states separated by high potential-energy barriers. The resulting free-energy differences were thus found to be zero within the error bars (Fig. 3(c)).

B. Five PNMT inhibitors in water

1. Testing the new scheme to estimate energy offsets

An RE-EDS simulation with the energy offsets determined using the new scheme ($\bar{E}^R_{i,RE}$) was compared to one with all energy offsets set to zero ($E^R_{i,0}$), one with the energy offsets set to the pairwise values taken from Ref. 10 ($E^R_{i,\text{pair}}$) and one with the energy offsets set to the average potential-energy

TABLE III. Free-energy differences ΔG_{ji} calculated using Eq. (2) for the five PNMT inhibitors **1**, **4**, **6**, **7**, and **10** in water from a RE-EDS simulation with pairwise energy offsets $E^R_{i,\text{pair}}$ taken from Ref. 10 and with energy offsets obtained with the new scheme, $\bar{E}^R_{i,RE}$ (see Table II). Results from TI calculations[26] and pairwise EDS simulations[10] are given as comparison. 21 s-values were logarithmically distributed between 1 and 0.001. The error bars given for the (RE-)EDS results are statistical uncertainties.[7] The error bars given for the TI results were estimated from block averaging.

Pair i-j	TI[26] ΔG_{ji} (kJ/mol)	EDS[10] ($E^R_{i,\text{pair}}$) ΔG_{ji} (kJ/mol)	RE-EDS ($E^R_{i,\text{pair}}$) ΔG_{ji} (kJ/mol)	RE-EDS ($\bar{E}^R_{i,RE}$) ΔG_{ji} (kJ/mol)
1-4	−3.4 ± 1.2	−2.8 ± 0.4	−2.8 ± 0.5	−3.3 ± 0.7
1-6	−37.8 ± 1.0	−36.7 ± 0.5	−37.3 ± 0.5	−37.8 ± 0.6
1-7	−343.0 ± 1.1	−341.5 ± 0.6	−348.6 ± 1.9	−344.6 ± 1.2
1-10	−123.5 ± 1.5	−129.3 ± 0.7	−127.4 ± 0.5	−128.9 ± 0.7
4-6			−34.5 ± 0.2	−34.6 ± 0.5
4-7	−340.4 ± 1.1	−338.6 ± 0.7	−345.8 ± 1.9	−341.4 ± 1.2
4-10	−120.0 ± 1.1	−125.9 ± 0.4	−124.6 ± 0.3	−125.6 ± 0.6
6-7			−311.3 ± 1.9	−306.8 ± 1.1
6-10	−84.7 ± 1.0	−91.4 ± 1.4	−90.1 ± 0.3	−91.0 ± 0.5
7-10			221.2 ± 1.9	215.8 ± 1.2

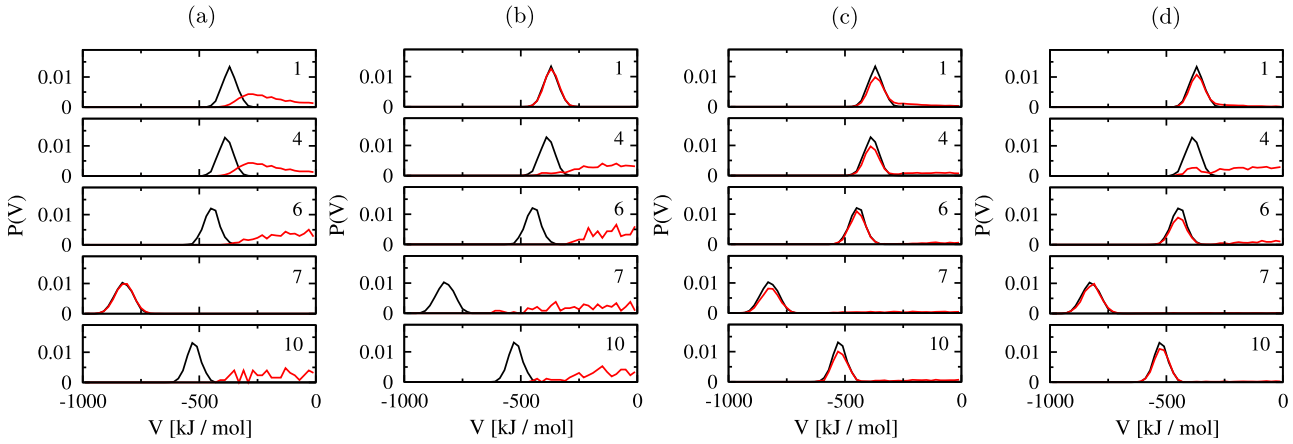

FIG. 5. Comparison of the potential-energy distributions V_i for the five ligands **1**, **4**, **6**, **7**, and **10** in water using the four different choices of energy offsets given in Table II. The black curves correspond to the potential-energy distribution obtained from 2-ns standard simulations of the individual ligands. The red lines correspond to the potential-energy distribution obtained from RE-EDS simulations at $s = 1$. (a) $E^R_{i,0}$. (b) $E^R_{i,\text{pot}}$. (c) $E^R_{i,\text{pair}}$. (d) $\bar{E}^R_{i,RE}$.

difference determined in 2-ns standard simulations of the individual ligands ($E^R_{i,\text{pot}}$) (Table II).

The results are shown in Fig. 4 in the form of the replica-exchange attempts in the first 2.5 ns, the state occupancy (i.e., how often a certain end state i was visited at $s = 1$), as well as the free-energy differences ΔG_{ji} between the five end states calculated using Eq. (2). When available, the estimated free-energy differences were compared with the values obtained by TI.[26] The numerical values of ΔG_{ji} are listed in Table III. The state occupancy was determined by comparing the potential energy of a configuration at time t, $V_i(\mathbf{r}(t))$, with the arithmetic mean of $V_i^{\text{non-EDS}}$ according to Eq. (10).

If all energy offsets were set to zero, essentially only ligand **7** was sampled at $s = 1$ (Fig. 4(a)). As ligand **1** corresponds to the core of ligand **7**, some configurations were favourable for ligand **1** as well. How well the relevant configurations of the end states were sampled can be seen in the potential-energy distributions (Fig. 5). If the low-energy configurations of an end state were sampled sufficiently, the corresponding potential-energy distribution is similar to the one observed in a standard simulation of the individual ligand. As can be seen in Fig. 5(a), only ligand **7** was sampled properly with $E^R_{i,0}$. The resulting free-energy differences deviated therefore from the values obtained by TI (data not shown). Introducing additional replicas with s-values in the gap region increased the replica-exchange acceptance rates in the gap region, but did not improve the sampling at $s = 1$ (Figs. S2 and S3 in the supplementary material), possibly due to leakage effects as explained in Fig. 1(b) in case of a one-dimensional potential surface. This suggests that an ample number of successful replica exchanges across the gap region is thus a necessary but not a sufficient condition for RE-EDS.

Similar results were observed for the RE-EDS simulation with the energy offsets set to the average potential energy

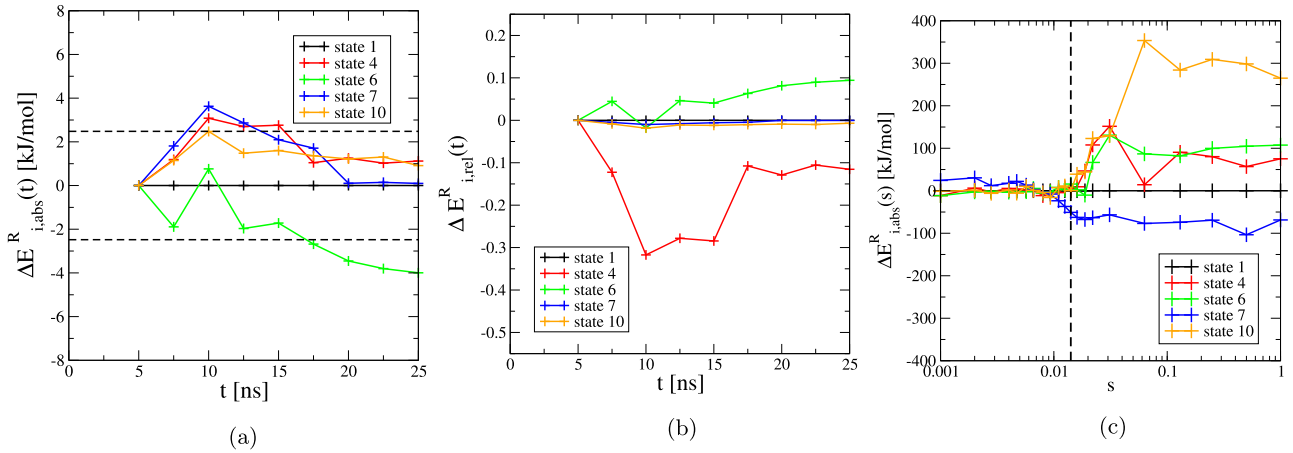

FIG. 6. Robustness analysis of the new scheme to estimate energy offsets from RE-EDS simulations. The RE-EDS simulation with the energy offsets set to zero ($E^R_{i,0}$) and optimised s-values was used for the analysis (system shown in Fig. S2 of the supplementary material). (a) Time evolution of the absolute energy-offset difference $\Delta E^R_{i,\text{abs}}(t)$. The dashed black lines indicate $\pm k_B T$. (b) Time evolution of the relative energy-offset difference $\Delta E^R_{i,\text{rel}}(t)$. (c) Difference between the averaged energy offset $\bar{E}^R_{i,RE}$ and the value estimated for a single s-value $E^R_{i,RE}(s)$. The vertical dashed line indicates the largest s-value with "undersampling" (i.e., $s \in U$), which contributes to the averaged value $\bar{E}^R_{i,RE}$ using the parameters $V_{th} = 0$ and $f_{th} = 0.5$.

TABLE IV. Energy offsets $\bar{E}^R_{i,RE}$ for nine and ten ligands **1**, (**2**), **3**, **4**, **5**, **6**, **7**, **8**, **9** and **10** in water. The estimated energy offsets of the smallest eight s-values (replicas) were averaged to yield $\bar{E}^R_{i,RE}$. The root-mean-square deviation of the average was computed as an error estimate.

Ligand i	9 states $\bar{E}^R_{i,RE}$ (kJ/mol)	10 states $\bar{E}^R_{i,RE}$ (kJ/mol)
1	0	0
2		−258.6 ± 15.5
3	−1.9 ± 7.5	−6.3 ± 6.6
4	−3.2 ± 6.2	−10.2 ± 5.7
5	7.4 ± 6.9	3.6 ± 6.2
6	−36.8 ± 6.2	−36.5 ± 4.2
7	−335.9 ± 10.5	−333.8 ± 16.8
8	−383.0 ± 19.7	−378.4 ± 22.2
9	−8.7 ± 5.4	−6.0 ± 4.2
10	−123.8 ± 5.4	−129.0 ± 5.7

(Fig. 4(b)). Even though the replica-exchange acceptance rate was significantly increased in the gap region, mainly ligand **1** was sampled (Fig. 5(b)), indicating that the energy offsets were estimated too negative relative to ligand **1** using this approach. This observation further supports the proposed presence of leakage effects for a non-optimal choice of the energy offsets.

Using the energy offsets determined in pairwise EDS simulations[10] on the other hand, all five end states were sampled with RE-EDS within 25 ns, and the free-energy differences agreed well with those obtained by TI (Fig. 4(c)). The potential-energy distributions of all five end states were found similar to the ones observed in standard simulations of the individual ligands (Fig. 5(c)).

The new scheme yielded energy offsets $\bar{E}^R_{i,RE}$ which were similar to the ones obtained from pairwise EDS (Table II). Consequently, an excellent agreement between the free-energy differences obtained by RE-EDS with $E^R_{i,\text{pair}}$ and by TI was found (Fig. 4(d)). All five end states were sampled within 25 ns. Although the low-energy configurations of ligand **4** were sampled less often compared to the RE-EDS simulation with $E^R_{i,pair}$ (Fig. 5(d)), no significant effect on the accuracy of the estimated free-energy differences was observed.

The RE-EDS simulations were carried out for 25 ns, but the analysis of the evolution of the free-energy differences as a function of time showed that a much shorter time frame would have been sufficient for this system (Fig. S4 in the supplementary material).

2. Robustness of the new scheme

To verify whether the chosen time frame of 2.5 ns is sufficient to obtain reliable energy-offset estimates, the absolute and relative differences in energy offsets as a function of time, $\Delta E^R_{i,\text{abs}}(t)$ and $\Delta E^R_{i,\text{rel}}(t)$, were calculated according to Eqs. (11) and (12) using the 25 ns run with optimised smoothness parameters $S^5_{0,\text{opt}}$ and all energy offsets were set to zero ($E^R_{i,0}$). The results are shown in Figs. 6(a) and 6(b). As the energy offsets were found to fluctuate only little (i.e., $\approx k_BT$), the energy offsets estimated from the 2.5-ns time frame can be considered converged. As mentioned in Section III A 2, the initial 2.5 ns were discarded as equilibration to avoid any bias due to initial configuration.

To test the definition of the undersampling region U, the difference in the estimated energy offsets $\Delta E^R_{i,\text{abs}}(s)$ according to Eq. (13) was computed for each replica using 2.5 ns of simulation data. The results are shown in Fig. 6(c). The vertical black line indicates the largest s-value still contributing to U. For $s \in S \setminus U$, the energy offsets $E^R_{i,RE}(s)$ start to deviate

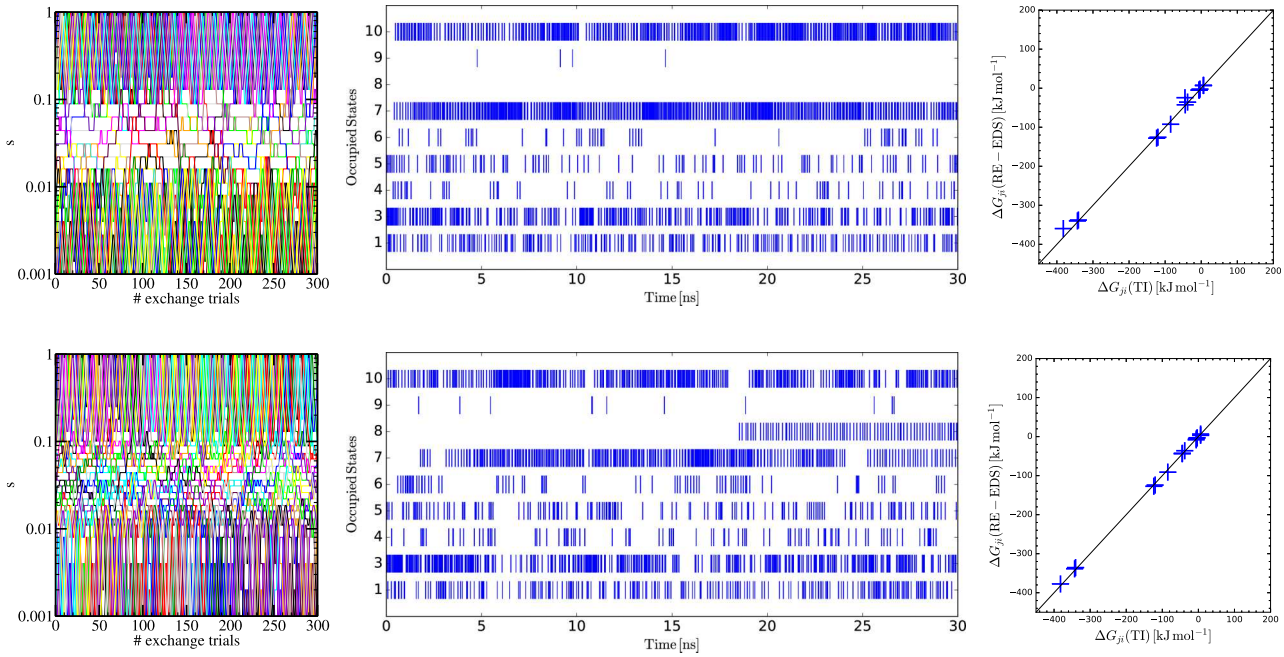

FIG. 7. RE-EDS simulation of the nine PNMT inhibitors **1**, **3**, **4**, **5**, **6**, **7**, **8**, **9**, and **10** in water with 21 logarithmically distributed s-values (top) and 24 manually optimised s-values (bottom). The energy offsets obtained using the new scheme $\bar{E}^R_{i,RE}$ (Table IV) were used in both simulations. From left to right: (i) Replica-exchange attempts in the first 3 ns, (ii) occupation of ligand i with respect to time t (i.e., $V_i < \bar{V}_i^{\text{non-EDS}}$), and (iii) comparison of the free-energy differences obtained by RE-EDS and TI.[26]

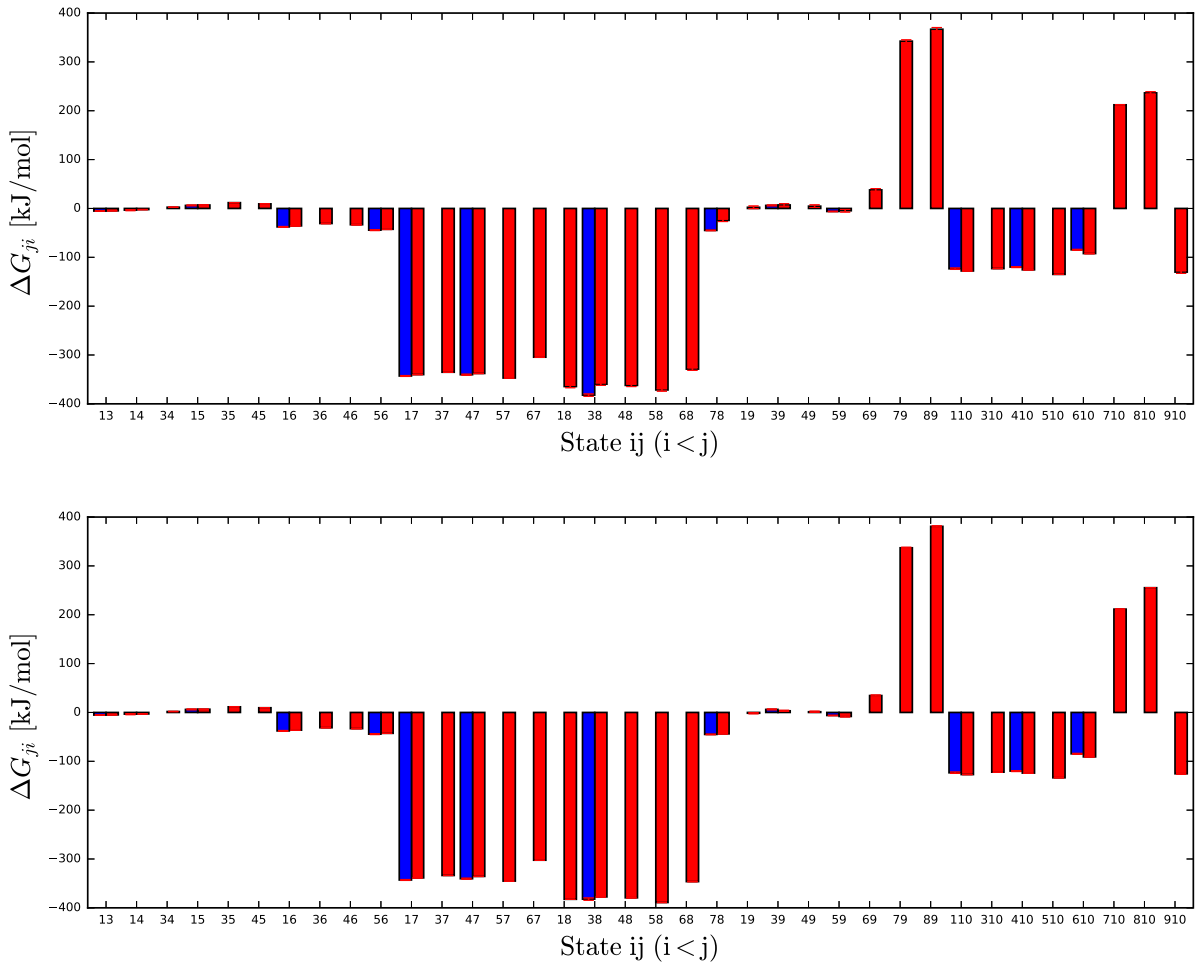

FIG. 8. Free-energy differences ΔG_{ji} obtained from a RE-EDS simulation of the nine ligands **1**, **3**, **4**, **5**, **6**, **7**, **8**, **9**, and **10** in water (red bars) with 21 logarithmically distributed s-values (top) and 24 manually optimised s-values (bottom). The energy offsets obtained using the new scheme $\bar{E}^R_{i,RE}$ (Table IV) were used in both simulations. The free-energy differences obtained from TI simulations[26] are shown for comparison (blue bars).

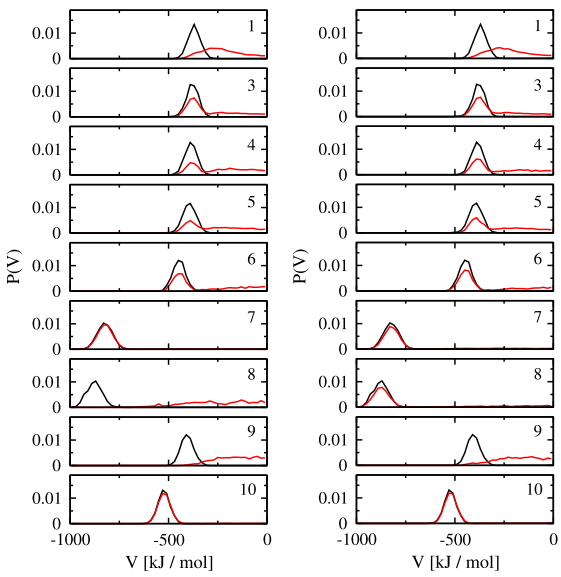

FIG. 9. Comparison of the potential-energy distribution for the nine ligands **1**, **3**, **4**, **5**, **6**, **7**, **8**, **9**, and **10** in water using the energy offsets obtained with the new scheme $\bar{E}^R_{i,RE}$ and 21 logarithmically distributed s-values (left) or 24 manually optimised s-values (right). The black curves correspond to the potential-energy distribution from 2-ns standard simulations of the individual ligands. The red curves correspond to the potential-energy distribution obtained from the RE-EDS replica at $s = 1$.

significantly from $\bar{E}^R_{i,RE}$ and the assumption that the energy offsets depend only weakly on s is either violated or not all end states were sampled. The latter certainly holds for $s = 1$ as can be seen from the results in Fig. 4(a). For the small s-values with undersampling ($s \in U$), the energy offsets do indeed depend only weakly on s for all end states except ligand **7**, which showed some dependence on $s \in U$.

Although the low-energy configurations of all end states were sampled better using the energy offsets obtained from pairwise EDS simulations $E^R_{i,pair}$ (Figs. 5(c) and 5(d)), the energy offsets obtained using the new scheme, $\bar{E}^R_{i,RE}$, were accurate enough to yield sufficient sampling of all end states at a potentially lower computational cost for their estimation.

C. Nine PNMT inhibitors in water

The new scheme to estimate energy offsets was applied to a system with nine PNMT inhibitors, i.e., ligands **1**, **3**, **4**, **5**, **6**, **7**, **8**, **9**, and **10** (Table IV). The results of the RE-EDS simulations with $\bar{E}^R_{i,RE}$ and 21 logarithmically or 24 manually distributed s-values are shown in Figs. 7 and 8. In the first case, ligand **8** was not sampled which can be seen in the state occupancy (Fig. 7) and the potential-energy distribution (Fig. 9). Hence, the resulting free-energy differences involving ligand **8** deviate

TABLE V. Free-energy differences ΔG_{ji} for the nine ligands **1**, **3**, **4**, **5**, **6**, **7**, **8**, **9**, and **10** in water obtained at replica $s = 1$ of the RE-EDS simulation with 21 logarithmically distributed s-values or 24 manually optimised s-values. The energy offsets determined with the new scheme $\bar{E}^{R}_{i,RE}$ (Table IV) were used in both simulations. The values obtained from TI calculation[26] are given for comparison. The errors given for the RE-EDS results are statistical uncertainties.[7]

		RE-EDS	
Pair i-j	TI ΔG_{ji} (kJ/mol)	ΔG_{ji}[a] (kJ/mol)	ΔG_{ji}[b] (kJ/mol)
1-3	−5.4 ± 0.4	−4.8 ± 0.3	−4.9 ± 0.3
1-4	−3.4 ± 1.2	−2.3 ± 0.4	−3.0 ± 0.4
1-5	6.2 ± 0.8	7.0 ± 0.4	6.6 ± 0.3
1-6	−37.8 ± 1.0	−35.6 ± 0.6	−36.2 ± 0.4
1-7	−343.0 ± 1.1	−340.1 ± 0.3	−338.7 ± 0.3
1-8		−364.5 ± 2.5	−382.5 ± 0.4
1-9		2.3 ± 2.7	−1.6 ± 1.1
1-10	−123.5 ± 1.5	−127.9 ± 0.3	−127.2 ± 0.3
3-4		2.5 ± 0.4	1.9 ± 0.4
3-5		11.8 ± 0.3	11.5 ± 0.3
3-6		−30.8 ± 0.6	−31.3 ± 0.4
3-7		−335.3 ± 0.2	−333.7 ± 0.3
3-8	−382.2 ± 2.4	−359.7 ± 2.5	−377.6 ± 0.4
3-9	6.2 ± 0.9	7.1 ± 2.67	3.3 ± 1.1
3-10		−123.1 ± 0.2	−122.2 ± 0.3
4-5		9.3 ± 0.4	9.6 ± 0.4
4-6		−33.3 ± 0.7	−33.2 ± 0.5
4-7	−340.4 ± 1.1	−337.8 ± 0.4	−335.6 ± 0.4
4-8		−362.2 ± 2.5	−379.5 ± 0.5
4-9		4.6 ± 2.7	1.4 ± 1.1
4-10	−120.0 ± 1.1	−125.6 ± 0.4	−124.1 ± 0.4
5-6	−44.4 ± 1.0	−42.6 ± 0.6	−42.8 ± 0.4
5-7		−347.1 ± 0.3	−345.2 ± 0.3
5-8		−371.5 ± 2.5	−389.1 ± 0.4
5-9	−6.2 ± 0.5	−4.6 ± 2.7	−8.2 ± 1.1
5-10		−134.9 ± 0.3	−133.7 ± 0.3
6-7		−304.5 ± 0.6	−302.5 ± 0.3
6-8		−328.9 ± 2.5	−346.3 ± 0.4
6-9		37.9 ± 2.7	34.6 ± 1.1
6-10	−84.7 ± 1.0	−92.3 ± 0.6	−91.0 ± 0.3
7-8	−45.0 ± 0.6	−24.4 ± 2.5	−43.8 ± 0.3
7-9		342.4 ± 2.7	337.1 ± 1.1
7-10		212.1 ± 0.2	211.5 ± 0.2
8-9		366.8 ± 3.6	380.9 ± 1.1
8-10		236.5 ± 2.5	255.4 ± 0.3
9-10		−130.2 ± 2.7	−125.6 ± 1.1

[a]21 logarithmically distributed s-values between 1 and 0.001.
[b]24 manually optimised s-values between 1 and 0.001.

from the values obtained by TI (Fig. 8 and Table V). However, the manual insertion of three replicas with s-values in the gap region improved the sampling considerably. Although the lowest-energy configurations were still not sampled perfectly for all ligands (Fig. 9), the sampling was sufficient to allow the accurate estimation of 36 free-energy differences from a single RE-EDS simulation (Fig. 8 and Table V). This illustrates that for a higher number of end states and larger differences between them, fine-tuning of the s-values (replicas) to increase the number of successful replica exchanges can be beneficial. This interpretation is supported by the evolution of the free-energy differences as a function of time, $\Delta G_{ji}(t)$, which shows for both s-distributions a fast initial convergence, but only with the optimised s-values it was possible to sample all nine end states within 30 ns and thus to obtain accurate ΔG_{ji} values (Fig. S5 in the supplementary material).

D. Ten PNMT ligands in water

The creation or deletion of a charge is generally a difficult change to estimate correctly in free-energy difference calculations. To test the limitations of the RE-EDS scheme, ligand **2** was included in the RE-EDS simulation. Ligand **2** contains a deprotonated carboxy substituent resulting in a net charge of zero, whereas all other ligands are positively charged (Fig. 2). As can be seen in Table IV, the energy offsets for ligands **1**, **3**–**10** are similarly when determined in the nine-state system and in the ten-state system. The energy offset of ligand **2**, however, was estimated to be more than 100 kJ mol^{-1} too positive compared to the pairwise energy offset reported in Ref. 10 (i.e., −379.7 or −373.3 kJ mol^{-1} relative to ligand **1**). In the subsequent RE-EDS simulation, ligand **2** was therefore sampled predominantly (Figs. S5 and S6 in the supplementary material). The reason for the too positive energy offset of ligand **2** is most likely due to the surrounding water. The energy offsets were estimated from small s-values where undersampling occurred, i.e., an unphysical intermediate configuration was sampled. The surrounding water interacts in these intermediate configurations with all ligands simultaneously. In the case of ligand **2**, this means that the surrounding water molecules cannot interact optimally with the negatively charged carboxy group. This can be seen in the radial distribution function (RDF) between the oxygen atoms of the carboxy group and the oxygen atoms of the water molecules (Fig. 10). In a standard simulation of ligand **2** in water, the peaks of the first solvation shells can be observed. The same peaks are missing in the RE-EDS replica with $s = 0.0057$ and energy offsets set to zero, which is used in the estimation of the energy offsets.

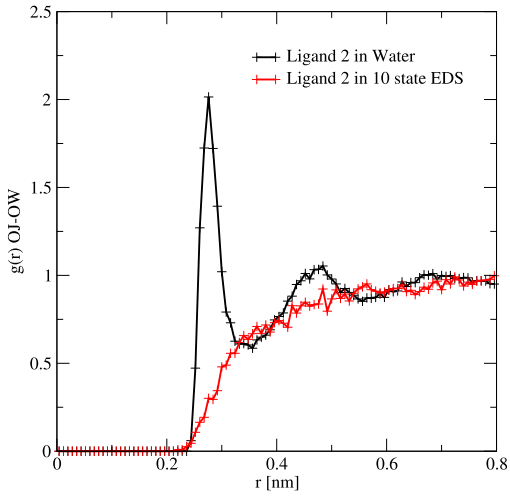

FIG. 10. Radial distribution function $g(r)$ between the oxygen atoms of the carboxy group of ligand **2** and the oxygen atoms of the surrounding water molecules. The black line corresponds to a 2-ns standard simulation of ligand **2** in water. The red line corresponds to the replica with $s = 0.0057$ of the RE-EDS simulation with ten ligands using energy offsets set to zero.

This finding illustrates nicely the limitations of the RE-EDS approach. In order to sample the end states sufficiently and efficiently in an RE-EDS simulation, the end states should not involve too large differences that require a substantial rearrangement of the surrounding solvent (or protein pocket). However, such end states can always be included via pairwise EDS simulations. In practical applications of binding free energy calculation with a large number of ligands, RE-EDS simulations could be applied for subsets of similar ligands connected by one or two ligands, in the same spirit as the lead optimisation mapper[5] used in large-scale FEP calculations.

V. CONCLUSION

RE-EDS as introduced by Lee *et al.* for constant-pH MD is an attractive approach to estimate multiple free-energy differences from a single simulation as it allows to reduce the complexity of the problem to choose optimal parameters for the EDS reference state. In constant-pH MD, the energy offsets can be obtained from the pH and pKa values, which limited the applicability of RE-EDS to these types of systems. In this study, a new scheme to estimate the energy offsets was introduced, which allows to generalise the RE-EDS method to any system. It was possible to extract the relevant information for N states in parallel from a short initial RE-EDS simulation with all energy offsets set to zero, without the need of a demanding iterative approach as used in previously proposed estimation schemes for EDS reference-state parameters.

RE-EDS simulation of the test system with five dis-/appearing water molecules in water, where the energy offsets are zero and the free-energy differences are known, revealed some characteristics of this setup. For small s-values with undersampling as well as for s-values close to one, the replica-exchange acceptance probability was close to one. In between, a gap region was observed with significantly decreased replica-exchange acceptance rates, indicating that in this region in s-space the potential-energy surface of the reference state changes. In addition, the existence of a finite gap region explains why it is possible to obtain an accurate estimate for the free energy differences at $s = 1$ for the given systems, without depending on higher s-values as implied by Eq. (A4). For the dis-/appearing water molecules in water, a broadening of the gap region was observed as a function of the number of end states. However, a generalisation of this observation towards more complex systems is difficult since other effects can possibly also have a significant impact on the width of the gap region, e.g., different energy offsets, the range of optimal pairwise s-values, distance restraints to keep multiple end states at the same position.

RE-EDS together with the new estimation scheme was applied for different sets of ten PNMT inhibitors in water. These ligands have been studied previously by TI and pairwise EDS. Excellent agreement with the previous results was obtained for up to nine ligands in a single RE-EDS simulation. The tenth ligand contains a deprotonated carboxy group and thus has a different net charge than the other ligands. This presents a limitation for the new energy-offset estimation scheme as the negatively charged carboxy substituent favours a substantially different solvent environment compared to other end states, which is not sampled in the reference state at small s-values. The resulting energy offset for this ligand was thus biased significantly, resulting in insufficient sampling of the other ligands in the subsequent RE-EDS production run. However, this is not a general limitation for RE-EDS as problematic energy offsets can always be estimated using the previously proposed pairwise procedure.

Furthermore, the results showed that the development of an automatic algorithm to distribute the smoothness parameters (i.e., replicas) is highly desirable in order to maximise the replica-exchange acceptance probabilities in the gap region, and at the same time minimise the number of replicas and thus lower the computational cost. Higher replica-exchange acceptance probabilities in the gap region would allow for a more efficient sampling of the reference state at $s = 1$. Future development will therefore focus on this aspect.

SUPPLEMENTARY MATERIAL

See supplementary material for the additional Figs. S1–S7 mentioned in the text.

ACKNOWLEDGMENTS

The authors gratefully acknowledge the financial support from the Swiss National Science Foundation (Grant No. 200021-159713) and by ETH Zürich (Grant No. ETH-08 15-1).

APPENDIX: FORCES FOR $s \to 0$ AND $s \to \infty$

The force acting on a particle k due to a reference-state potential Eq. (1) can be written as[9]

$$\vec{f}_k(\mathbf{r}, s, \vec{E}^R) = -\frac{\partial V_R(\mathbf{r})}{\partial \mathbf{r}_k} \tag{A1}$$

$$= \sum_{i=1}^{N} \left\{ \left(\sum_{j=1,\ j\neq i}^{N} e^{-\beta s \left(V_j(\mathbf{r}) - V_i(\mathbf{r}) - E_j^R + E_i^R \right)} + 1 \right)^{-1} \times \left(-\frac{\partial V_i(\mathbf{r})}{\partial \mathbf{r}_k} \right) \right\}. \tag{A2}$$

If V_j, V_i, and $\vec{E}^R$ are assumed to be finite, it follows immediately for $s \to 0$

$$\lim_{s\to 0} \vec{f}_k(\mathbf{r}, s, \vec{E}^R) = -\frac{1}{N} \sum_{i=1}^{N} \left(\frac{\partial V_i(\mathbf{r})}{\partial \mathbf{r}_k} \right). \tag{A3}$$

For $s \to \infty$, we further restrict our assumptions to $\vec{E}^R \stackrel{!}{=} 0$ and $V_m(\mathbf{r}) < V_i(\mathbf{r})$, for a given configuration $\mathbf{r}$ without loss of generality,

$$\lim_{s\to\infty} \vec{f}_k(\mathbf{r}, s) = \sum_{i=1}^{N} \left\{ \frac{1}{\sum_{j=1,\ j\neq i}^{N} \lim_{s\to\infty} e^{-\beta s (V_j(\mathbf{r}) - V_i(\mathbf{r}))} + 1} \times \left(-\frac{\partial V_i(\mathbf{r})}{\partial \mathbf{r}_k} \right) \right\}$$

$$= \sum_{i=1}^{N} \delta_{im} \left(-\frac{\partial V_i(\mathbf{r})}{\partial \mathbf{r}_k} \right) = -\frac{\partial V_m(\mathbf{r})}{\partial \mathbf{r}_k}. \tag{A4}$$

Hence, in the limit of $s \to \infty$ the force on particle k is equivalent to the simulation of V_m for which the configuration $\mathbf{r}$ is energetically most favourable.

[1]C. Chipot and A. Pohorille, *Free Energy Calculations* (Springer-Verlag, Berlin, Heidelberg, 2007).
[2]C. D. Christ, A. E. Mark, and W. F. van Gunsteren, J. Comput. Chem. **31**, 1569 (2010).
[3]J. G. Kirkwood, J. Chem. Phys. **3**, 300 (1935).
[4]R. W. Zwanzig, J. Chem. Phys. **22**, 1420 (1954).
[5]S. Liu, Y. Wu, T. Lin, R. Abel, J. P. Redmann, C. M. Summa, V. R. Jaber, N. M. Lim, and D. L. Mobley, J. Comput.-Aided Mol. Des. **27**, 755 (2013).
[6]C. D. Christ and W. F. van Gunsteren, J. Chem. Phys. **126**, 184110 (2007).
[7]C. D. Christ and W. F. van Gunsteren, J. Chem. Phys. **128**, 174112 (2008).
[8]C. D. Christ and W. F. van Gunsteren, J. Chem. Theory Comput. **5**, 276 (2009).
[9]C. D. Christ and W. F. Van Gunsteren, J. Comput. Chem. **30**, 1664 (2009).
[10]S. Riniker, C. D. Christ, N. Hansen, A. E. Mark, P. C. Nair, and W. F. van Gunsteren, J. Chem. Phys. **135**, 024105 (2011).
[11]U. H. E. Hansmann, Chem. Phys. Lett. **281**, 140 (1997).
[12]Y. Sugita, A. Kitao, and Y. Okamoto, J. Chem. Phys. **113**, 6042 (2000).
[13]C. J. Woods, J. W. Essex, and M. A. King, J. Phys. Chem. B **107**, 13703 (2003).
[14]J. Lee, B. T. Miller, A. Damjanovic, and B. R. Brooks, J. Chem. Theory Comput. **10**, 2738 (2014).
[15]J. Lee, B. T. Miller, A. Damjanovic, and B. R. Brooks, J. Chem. Theory Comput. **11**, 2560 (2015).
[16]K.-K. Han, Phys. Lett. A **165**, 28 (1992).
[17]Y.-G. Chen and G. Hummer, J. Am. Chem. Soc. **129**, 2414 (2007).
[18]Y. Sugita and Y. Okamoto, Chem. Phys. Lett. **314**, 141 (1999).
[19]N. Schmid, C. D. Christ, M. Christen, A. P. Eichenberger, and W. F. van Gunsteren, Comput. Phys. Commun. **183**, 890 (2012).
[20]S. Riniker, C. D. Christ, H. S. Hansen, P. H. Hünenberger, C. Oostenbrink, D. Steiner, and W. F. van Gunsteren, J. Phys. Chem. B **115**, 13570 (2011).
[21]C. Oostenbrink, A. Villa, A. E. Mark, and W. F. Van Gunsteren, J. Comput. Chem. **25**, 1656 (2004).
[22]H. J. C. Berendsen, J. P. M. Postma, W. F. van Gunsteren, and J. Hermans, "Interaction models for water in relation to protein hydration," in *Intermolecular Forces*, edited by B. Pullman (Reidel, Dordrecht, The Netherlands, 1981), pp. 331–342.
[23]I. G. Tironi, R. Sperb, P. E. Smith, and W. F. van Gunsteren, J. Chem. Phys. **102**, 5451 (1995).
[24]T. N. Heinz, W. F. van Gunsteren, and P. H. Hünenberger, J. Chem. Phys. **115**, 1125 (2001).
[25]H. J. Berendsen, J. V. Postma, W. F. van Gunsteren, A. DiNola, and J. Haak, J. Chem. Phys. **81**, 3684 (1984).
[26]P. C. Nair, A. K. Malde, and A. E. Mark, J. Chem. Theory Comput. **7**, 1458 (2011).
[27]A. P. Eichenberger, J. R. Allison, J. Dolenc, D. P. Geerke, B. A. C. Horta, K. Meier, C. Oostenbrink, N. Schmid, D. Steiner, D. Wang, and W. F. van Gunsteren, J. Chem. Theory Comput. **7**, 3379 (2011).